# IKONOS GEOMETRIC ACCURACY VALIDATION

J. Grodecki, G. Dial

Space Imaging, 12076 Grant Street, Thornton, CO 80241, U.S.A. (jgrodecki, gdial)@spaceimaging.com

**KEY WORDS:** Photogrammetry, Calibration, Camera, Satellite, IKONOS, Accuracy, Geometric, High resolution

**ABSTRACT:**

Since its launch in September of 1999, the IKONOS satellite has been consistently providing high quality 1-meter panchromatic and 4-meter multispectral images. Accurate interior and exterior orientation enable IKONOS to achieve high geometric accuracy with or without ground control. Exterior orientation is determined by on-board GPS receivers, star trackers, gyros, and interlock angles. Post-processing of GPS data with software incorporating sophisticated filtering and orbital modeling algorithms results in accurate ephemeris. Kalman filtering of gyro and star tracker data results in optimal combination of lower frequency star tracker attitude data exhibiting high absolute accuracy with high frequency gyro data being very accurate over short time intervals. Interlock angles relate the attitude and the camera coordinate systems and have been calibrated both pre-launch and in-flight. Initial interior orientation parameter values were determined by pre-launch measurements and later refined by in-flight calibration. In this paper, we shall first demonstrate the high accuracy of such calibrations based on test range data. Later, we shall quantify the geometric accuracy of the IKONOS camera using large IKONOS stereo image blocks with and without ground control, thus validating the exterior and the interior orientation calibrations.

## 1. INTRODUCTION

The initial post-launch IKONOS geometric accuracy was verified during the On-Orbit Acceptance Test (OOAT), using the San Diego test range consisting of 140 ground control points (GCP) over a 22 by 22km area [Grodecki and Dial, 2001]. The OOAT results indicated that the absolute horizontal and vertical accuracy of uncontrolled IKONOS stereo images – block adjusted without GCPs – was better than 6 m. The absolute horizontal and vertical accuracy of GCP-controlled stereo images was determined to be better than 2 m.

The initial IKONOS interior and exterior orientation parameters were further refined by in-flight calibrations. The present paper describes the results of such calibrations, and illustrates the resulting geometric accuracy of the IKONOS satellite using large stereo image blocks with and without ground control.

## 2. IKONOS OVERVIEW

Launched in September of 1999, IKONOS became the world's first commercial high-resolution imaging satellite. It was placed in a 680 km sun synchronous orbit with descending node crossing at about 10:15 am local solar time and the orbital inclination of 98 degrees.

The IKONOS satellite simultaneously collects imagery in four multispectral bands and a single panchromatic band with 11-bit resolution. The IKONOS multispectral bands approximate Landsat bands 1 through 4.

For panchromatic images the ground sampling distance (GSD) of the IKONOS sensor is 0.82 m at nadir. GSD of multispectral images is four times that of panchromatic images, i.e., 3.28 m at nadir. At 26 degrees off nadir the GSD is 1 m for panchromatic and 4 m for multispectral images. Nominal swath width at 1 m GSD is 13 km.

At 40 degrees latitude the revisit time is 2.9 days at 1 m GSD and 1.5 days at 1.5 m GSD. The revisit times are shorter for higher latitudes and longer for latitudes closer to the equator.

Unlike Landsat, which only images at nadir, and SPOT, which has a rotating mirror permitting only the side-to-side image acquisition, the IKONOS satellite is a fully agile satellite. IKONOS can be rotated to any off-nadir angle to acquire an image to the side, forward, or aft of the current satellite position.

Detailed overviews of the IKONOS satellite may be found in [Dial 2001], [Dial et al., 2001], and [Grodecki and Dial, 2001].

## 3. INTERIOR AND EXTERIOR ORIENTATION

Interior and exterior orientation of the IKONOS satellite are derived from sophisticated attitude and ephemeris determination systems, a stable optical assembly, and a solid state focal plane, enabling IKONOS to achieve high geometric accuracy with or without ground control.

### 3.1 Interior orientation

The IKONOS solid state focal plane array consists of multiple panchromatic and multispectral line arrays. The detectors in each line array are rigidly attached to the focal plane in a stable thermal-mechanical environment.

The interior orientation of the IKONOS camera is described by the Field Angle Map (FAM). FAM allows one to determine the line-of-sight vector in the camera coordinate system for each image pixel. Combining satellite attitude, interlock angles, and the Field Angle Map allows calculation of the pointing direction of every image pixel.

### 3.2 Exterior orientation

Exterior orientation comprises the satellite attitude and ephemeris, and is determined by the on-board GPS receivers, star trackers, gyros, and interlock angles.

The satellite ephemeris and the camera position for each image line results from post-processing of GPS data with software incorporating sophisticated filtering and orbital modeling algorithms.

The satellite attitude is measured by on-board star trackers and gyros. Kalman filtering of gyro and star tracker data results in optimal combination of lower frequency star tracker attitude data exhibiting high absolute accuracy with high frequency gyro data being very accurate over short time intervals.

Interlock angles relate the satellite attitude to the camera orientation angles. The initial interlock angles were determined by pre-launch assembly measurements. They also are being periodically refined by in-flight calibration.

### 4. IKONOS GEOMETRIC CALIBRATIONS

### 4.1 FAM Calibration

Initial interior orientation (FAM) parameter values were determined by pre-launch lab measurements and later refined by in-flight calibration. The results of the in-flight FAM calibration are described in this section.

The main goal of the in-flight FAM calibration was to reduce various interior orientation systematic errors. Additional objectives were to improve panchromatic-multispectral registration and re-estimate interlock angles.

The in-flight FAM calibration was performed over the Denver test range consisting of 33 GPS-surveyed GCPs.

The post-FAM-calibration residual errors are shown in Figure 1 against the GCP layout. No significant systematic error pattern can be observed and most of the residual errors are within ±1 pixel, which is the expected combined GCP and pick accuracy, thus validating that the main objective of the in-flight FAM calibration was successfully accomplished.

Panchromatic-multispectral misregistration was reduced to a small fraction of a panchromatic pixel resulting in better quality pan-sharpened images.

The FAM parameters determined over the Denver test range were later verified over the Southern test range located in Australia. The Southern test range comprises a 100km by 100km area with over 200 GCPs. The resulting residual errors are shown in Figure 2. As before, no significant systematic error pattern can be observed in the residual plot.
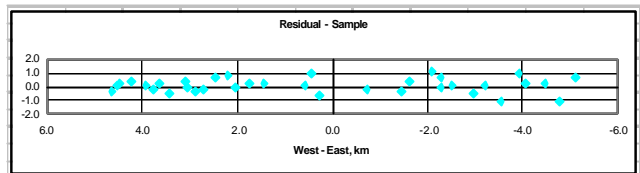




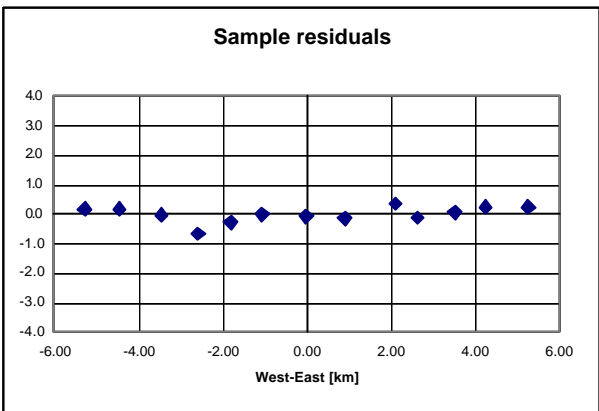Figure 1. Post-FAM-calibration residual errors against the Denver test range.



Figure 2. Post-FAM-calibration residual errors over the Southern test range.

### 4.2 Interlock Calibration

To improve post-FAM-calibration interlock accuracy a set of independent images, taken repeatedly over the Space Imaging MTF target shown in Figure 3 below, was used for the in-flight interlock calibration.
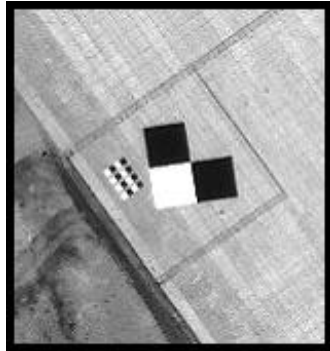
Figure 3. Space Imaging MTF Target

The interlock angle errors for each image were determined by the IKONOS ground station block adjustment with the MTF GCP. The resulting time series of roll and pitch interlock errors are shown below in Figure 4 and 5, respectively.
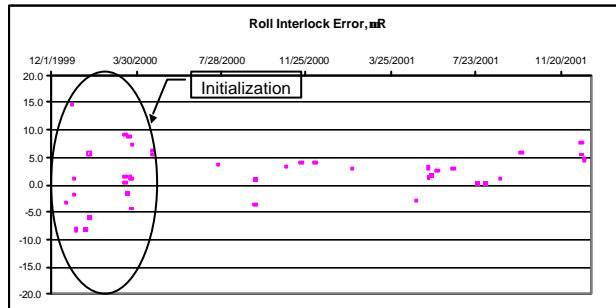


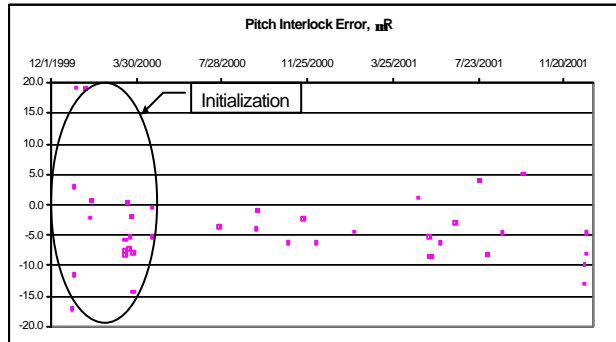Figure 4. Time series of roll interlock errors.



Figure 5. Time series of roll interlock errors.

Excluding the initialization period directly following the launch of the IKONOS satellite, the adjustments to the interlock angles were computed as $\Delta\text{Pitch} = +4.5\ \mu R$ and $\Delta\text{Roll} = -2.5\ \mu R$. Figure 6 shows the resulting post-interlock-calibration error distribution.
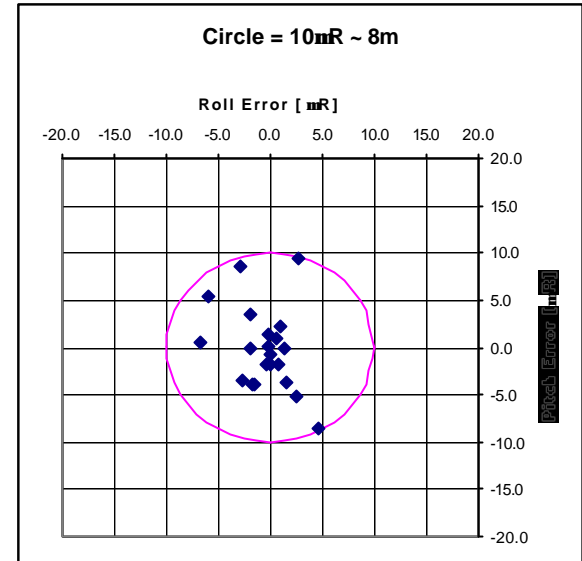


Figure 6. Post-interlock-calibration error distribution.

## 5. VALIDATION

A Space Imaging project located in Mississippi, with 6 stereo strips and a large number of well-distributed GCPs as shown in Figure 7, was selected to validate the FAM and interlock calibrations.
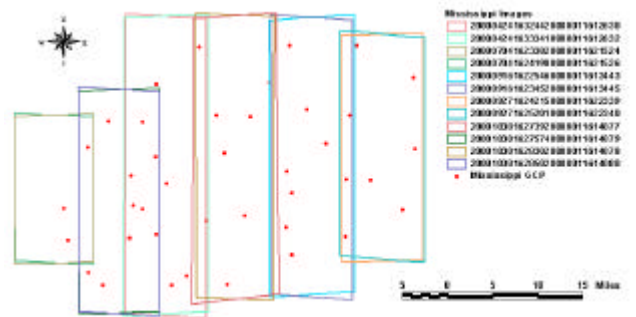


Figure 7. Image and GCP Layout for Mississippi Project

Each of the 12 source images was produced as a georectified image with rational polynomial camera models (RPC). The images were then loaded onto a SOCET SET® workstation running the custom-developed RPC block adjustment model, described in more detail in [Dial and Grodecki, 2002a] and [Grodecki and Dial, 2002], illustrated below by equations (1) and (2):

$$L = R_L(\boldsymbol{f}, \boldsymbol{l}, h) + a_o + a_L L_n + \boldsymbol{e}_L \qquad (1)$$
$$S = R_S(\boldsymbol{f}, \boldsymbol{l}, h) + b_o + b_L L_n + \boldsymbol{e}_S \qquad (2)$$

where

| | |
|---|---|
| $(\boldsymbol{f}, \boldsymbol{l}, h) =$ | latitude, longitude, and height, |
| $L, S =$ | measured image line and sample coordinates, |

**IKONOS GEOMETRIC ACCURACY VALIDATION**

$L_n$ = approximate fixed value for the true image line coordinate,

$R_L$, $R_S$ = nominal ground to image RPC functions for line and sample, provided with the IKONOS images,

$a_o$, $b_o$ = adjustable bias parameters for line and sample,

$a_L$, $b_L$ = adjustable drift parameters for line and sample, and

$\boldsymbol{e}_L$, $\boldsymbol{e}_S$ = random unobservable line and sample errors.

As shown in [Dial and Grodecki, 2002a], bias parameters ($a_o$, $b_o$) account for bias errors in satellite attitude or ephemeris, while drift parameters ($a_L$, $b_L$) model time proportional errors in satellite attitude.

Multiple well-distributed tie points were measured along the edges of the images. Ground control points were selectively changed between control and check points to quantify block adjustment accuracy as a function of a number and distribution of GCPs.

As demonstrated by the *a posteriori* IKONOS error analysis in [Dial and Grodecki, 2002b], the *a priori* standard deviations for $a_o$ and $b_o$ should be 4 pixels, while the *a priori* standard deviations for $a_L$ and $b_L$ should be 50 ppm. Accordingly, these were the *a priori* standard deviations used in all block adjustments presented in this section.

## 5.1 FAM Validation

The estimated FAM parameters and the adjustments to the interlock angles, resulting from the in-flight FAM calibration, were implemented in the IKONOS ground station and used to generate all 6 Mississippi stereo strips.

The block adjustment results presented in Table 1 were obtained using a simple two-parameter, offset only, model with *a priori* values for $a_0$ and $b_0$ of 0 pixels and *a priori* σ of 4 pixels. The corresponding residual plots are shown in Figures 8, 9 and 10, where red vertical arrows depict vertical errors, while black arrows represent horizontal errors. It is seen that most of the errors affecting IKONOS are bias errors that can be eliminated by inclusion of a single GCP.

Table 1. Post-FAM-calibration Mississippi Block Adjustment Results using the Two-Parameter Model

| GCP | Average Error l | Average Error f | Average Error h | CE90 | LE90 |
|---|---|---|---|---|---|
| None | -5.3 m | 6.2 m | 0.0 m | 8.5 m | 3.0 m |
| 1 | -2.8 m | 1.6 m | -1.4 m | 3.9 m | 3.1 m |
| All | 0.0 m | 0.0 m | 0.0 m | 1.4 m | 0.7 m |

To model attitude drifts, the block adjustment was re-run using the four-parameter model, offsets plus drifts, as shown in equations (1) and (2). The *a priori* values for $a_o$ and $b_o$ were 0 pixels and *a priori* σ were 4 pixels. The *a priori* values for $a_L$ and $b_L$ of 0 ppm and *a priori* σ of 50 ppm. The results of the adjustments are presented in Table 2. The corresponding residual plots are virtually identical to the ones shown in Figures 8, 9 and 10.

Table 2. Post-FAM-calibration Mississippi Block Adjustment Results using the Four-Parameter Model

| GCP | Average Error l | Average Error f | Average Error h | CE90 | LE90 |
|---|---|---|---|---|---|
| None | -5.0 m | 6.1 m | 1.3 m | 8.3 m | 3.1 m |
| 1 | -2.6 m | 1.5 m | -0.5 m | 3.8 m | 2.9 m |
| All | 0.0 m | 0.0 m | 0.0 m | 1.3 m | 0.5 m |

As illustrated by the block adjustment results presented above, inclusion of drift parameters slightly improved the resulting horizontal and vertical accuracies. As shown in Table 3, in all cases the estimated drifts were below 96 ppm (43 ppm RMS) for line and less than 57 ppm (30 ppm RMS) for sample. It should be noted that many of the estimated drift parameters turned out to be statistically insignificant.

Table 3. Estimated drift parameters

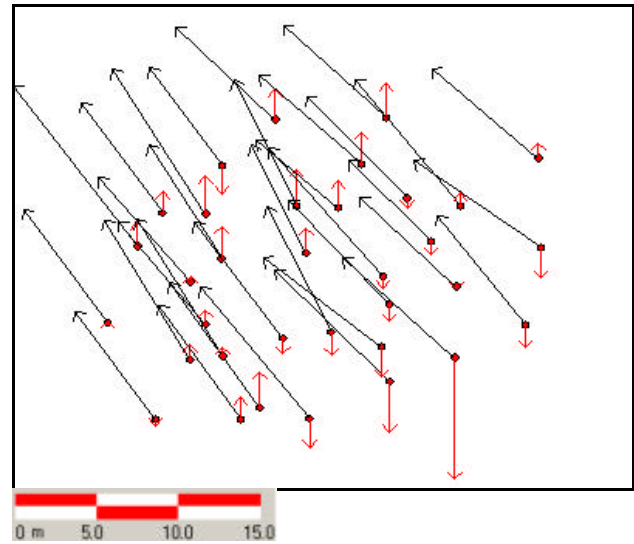| GCP | Min $a_L$ [ppm] | Max $a_L$ [ppm] | RMS $a_L$ [ppm] | Min $b_L$ [ppm] | Max $b_L$ [ppm] | RMS $b_L$ [ppm] |
|---|---|---|---|---|---|---|
| None | -48 | 35 | 27 | -33 | 36 | 21 |
| 1 | -59 | 20 | 29 | -41 | 28 | 22 |
| All | -96 | 65 | 43 | -37 | 57 | 30 |



Figure 8. Horizontal and Vertical Errors without GCPs
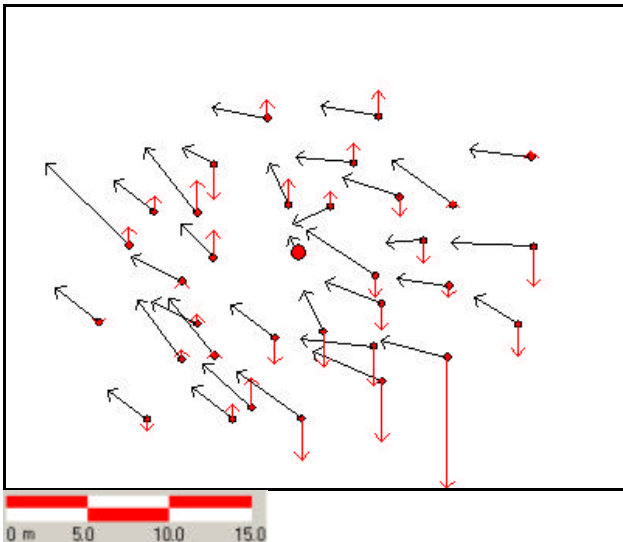
**IKONOS GEOMETRIC ACCURACY VALIDATION**

Figure 9. Horizontal and Vertical Errors with 1 GCP in the Center.
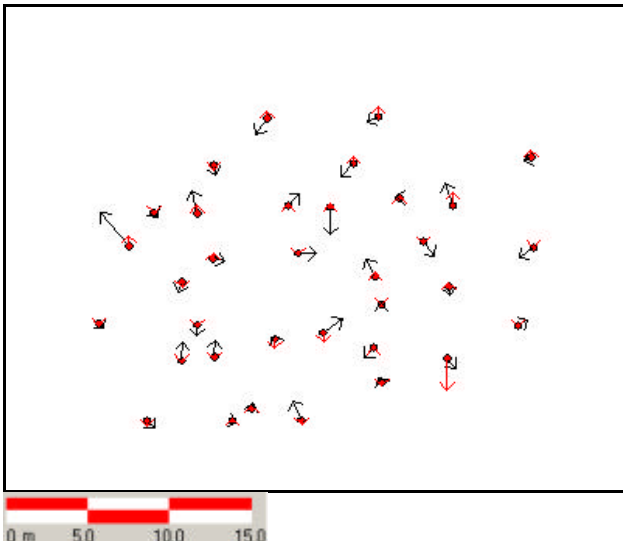


Figure 10. Horizontal and Vertical Errors with All GCPs

It is seen in Figure 10 that no systematic residual error trends can be observed in the block adjustment results for the case with all GCPs, thus validating the in-flight FAM calibration results. However, for the case with no GCPs (see Figure 8) large horizontal biases are observed indicating the need for the interlock angle improvement. The next section will show that the new interlock angles resulting from the in-flight interlock calibration, described in Section 4.2, indeed significantly reduce these errors.

### 5.2 Interlock Validation

The estimated interlock angles, resulting from the in-flight interlock angle calibration, were combined with the new FAM parameters, resulting from the in-flight FAM calibration, and used to re-generate all 6 Mississippi stereo strips.

The block adjustment results presented in Table 4 were obtained using a simple two-parameter, offset only, model and the same *a priori* values and weights as before. The corresponding residual plots are shown in Figures 11, 12 and 13.

Table 4. Mississippi Block Adjustment Results using the Two-Parameter Model – Post-interlock-calibration

| GCP | Average Error l | Average Error f | Average Error h | CE90 | LE90 |
|-----|-----|-----|-----|-----|-----|
| None | -3.1 m | 2.6 m | -0.5 m | 4.6 m | 2.9 m |
| 1 | -1.7 m | 0.8 m | -0.2 m | 2.8 m | 2.9 m |
| All | 0.0 m | 0.0 m | 0.0 m | 1.2 m | 0.7 m |

As before, to model attitude drifts, the block adjustment was re-run using the four-parameter model, offsets plus drifts, as shown in equations (1) and (2). The same *a priori* constraints were used as previous examples. The results of the adjustments are presented in Table 5. The corresponding residual plots are virtually identical to the ones shown in Figures 11, 12 and 13.

Table 5. Mississippi Block Adjustment Results using the Four-Parameter Model – Post-interlock-calibration

| GCP | Average Error l | Average Error f | Average Error h | CE90 | LE90 |
|-----|-----|-----|-----|-----|-----|
| None | -2.9 m | 2.5 m | 1.0 m | 4.4 m | 2.7 m |
| 1 | -1.5 m | 0.7 m | 0.0 m | 2.7 m | 2.5 m |
| All | 0.0 m | 0.0 m | 0.0 m | 1.1 m | 0.5 m |

As illustrated by the block adjustment results presented in Tables 4 and 5, inclusion of drift parameters slightly improved the resulting horizontal and vertical accuracies. The ranges for the estimated drift parameters are given in Table 6.

Table 6. Estimated drift parameters

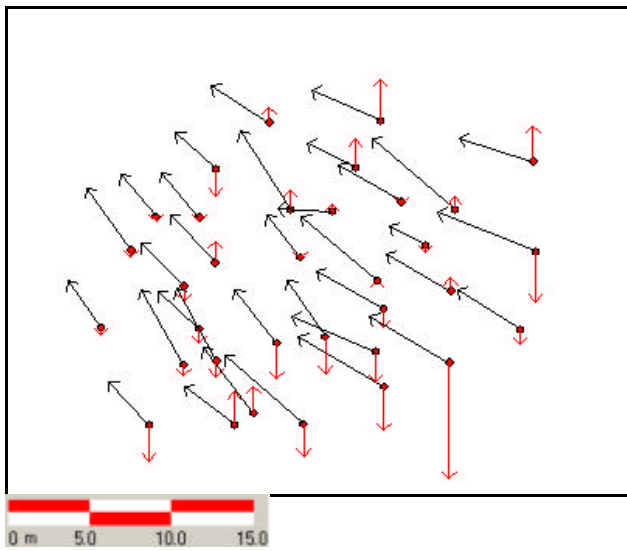| GCP | Min $a_L$ [ppm] | Max $a_L$ [ppm] | RMS $a_L$ [ppm] | Min $b_L$ [ppm] | Max $b_L$ [ppm] | RMS $b_L$ [ppm] |
|-----|-----|-----|-----|-----|-----|-----|
| None | -47 | 35 | 21 | -28 | 48 | 19 |
| 1 | -47 | 29 | 21 | -33 | 44 | 19 |
| All | -87 | 67 | 40 | -20 | 54 | 21 |

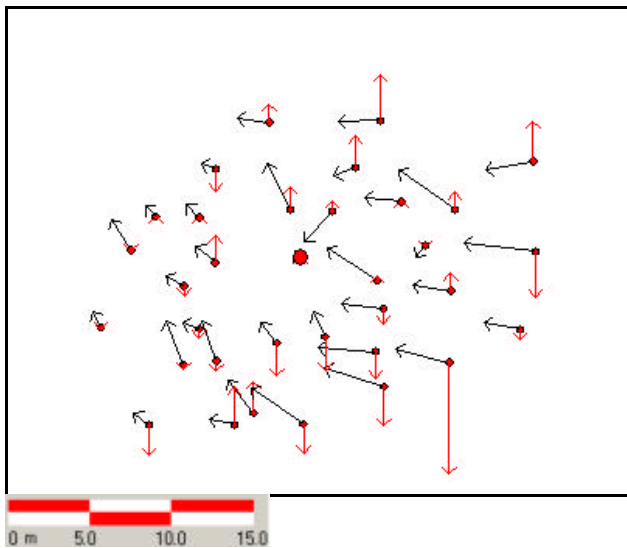Figure 11. Horizontal and Vertical Errors without GCPs



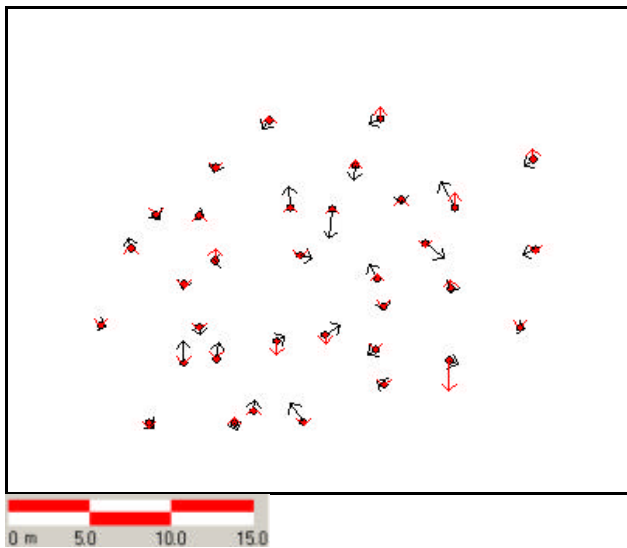Figure 12. Horizontal and Vertical Errors with 1 GCP in the Center.



Figure 13. Horizontal and Vertical Errors with All GCPs

It is seen that for the case with no GCP, the large horizontal bias errors shown in Figure 8 were significantly reduced. It is also seen that for the case with 1 GCP both the horizontal and the vertical errors are smaller than previously. The presented results unambiguously validate the in-flight interlock calibration results.

## 6. CONCLUSIONS

Interior and exterior orientation of the IKONOS satellite are derived from sophisticated attitude and ephemeris determination systems, a stable optical assembly, and a solid state focal plane, enabling IKONOS to achieve high geometric accuracy with or without ground control.

The initial IKONOS interior and exterior orientation parameters have been further refined by in-flight calibrations using test range data. The present paper demonstrates the high accuracy of such calibrations.

Finally, the results of in-flight calibrations have been successfully validated using large IKONOS stereo image blocks with and without ground control demonstrating high geometric accuracy of IKONOS satellite.

## 7. REFERENCES

Dial, Gene (2001). "IKONOS Overview." *Proceedings of the High-Spatial Resolution Commercial Imagery Workshop,* Washington DC, March 19-22, 2001.

Dial, Gene, Laurie Gibson, and Rick Poulsen (2001). "IKONOS Satellite Imagery and its Use in Automated Road Extraction" in Baltsavias, Gruen, and Gool, *Automatic Extraction of Man-Made objects from Aerial and Space Images (III)*, A.A. Balkema Publishers, 2001.

Dial, Gene and Jacek Grodecki (2002a). "Block Adjustment with Rational Polynomial Camera Models." *Proceedings of ASPRS 2002 Conference*, Washington, DC, April 22-26, 2002.

Dial, Gene and Jacek Grodecki (2002b). "IKONOS Accuracy without Ground Control." *Proceedings of ISPRS Comission I Mid-Term Symposium*, Denver, CO, November 10-15, 2002.

Grodecki, Jacek and Gene Dial (2001). "IKONOS Geometric Accuracy." *Proceedings of Joint Workshop of ISPRS Working Groups I/2, I/5 and IV/7 on High Resolution Mapping from Space 2001,* University of Hannover, Hannover, Germany, Sept 19-21, 2001.

Grodecki, Jacek and Gene Dial (2002). "Block Adjustment of High-Resolution Satellite Images Described by Rational Polynomials." Accepted for publication in PE&RS, 2002.

**IKONOS GEOMETRIC ACCURACY VALIDATION**